Hindawi
Journal of Sensors
Volume 2021, Article ID 5524057, 14 pages
https://doi.org/10.1155/2021/5524057

Research Article

Analysis of Surface Deformation in East Dongting Lake Based on 2016-2019 Sentinel-1A Dataset

Heng Zhang[1,2] **Qian Sun**[1,2] **and Jun Hu**[3]

[1]*College of Geographic Science, Hunan Normal University, Changsha 410081, China*
[2]*Key Laboratory of Geospatial Big Data Mining and Application, Hunan Normal University, Changsha 410081, China*
[3]*School of Geosciences and Info-Physics, Central South University, Changsha 410083, China*

Correspondence should be addressed to Qian Sun; sandra@hunnu.edu.cn

Received 8 February 2021; Revised 29 March 2021; Accepted 19 April 2021; Published 3 May 2021

Academic Editor: Hyung-Sup Jung

In this study, 84 scenes Sentinel-1A satellite datasets from October 2016 to September 2019 were used to analyze surface deformation in East Dongting Lake, China, by employing the small baseline subset interferometric synthetic aperture radar (SBAS-InSAR) method. The data are divided into two seasons, i.e., the flood and dry seasons. It was suggested that the surface deformation is related to the distribution of the river network and water flow activities. During the dry season, the water flow is active along the internal river, scouring the surrounding soil. During the flood season, the water flow basically occurs around the external drainage network. By qualitatively comparing surface deformation and precipitation changes as well as changes in soil erosion, it is found that the deformation was highly related to soil erosion and seasonal precipitation. The precipitation in the flood period is heavy than that in the dry season. Therefore, the runoff with amount silt will scour the soil in the passing area, resulting obvious surface deformation. During the dry period, surface deformation is smaller due to the less precipitation.

1. Introduction

Surface deformation in lake region associated with mud and sand is a common problem in the world nowadays, seriously threatening agriculture irrigation, natural resources protection, and ecosystem environments regulation [1, 2]. Lake region's surface deformation mainly includes two processes. One is surface settlement, which is caused by score and erosion of flowing water to soft soil in the uppermost layer of the lake region. The surface soil flows to other areas with flowing water, thus, causing surface settlement in the passing area. Another deformation is surface sedimentation, which is due to the increase of sediment content brought by the flowing water. Due to gravity and sedimentation, silt deposits on the surface and raises the lake bed. Lake area will decrease due to sedimentation. Continuous silt uplift of the river bed also brings huge challenges to flood control. Over the past years, numerous mud blockage river events had been reported in many lakes around the world [3]. In China, more than 5 billion tons of mud and sand are lost to drainage network each year, which causes the silting of rivers, raising of river beds, silting of reservoirs, and reduction of the reservoir capacity [4]. Therefore, surface deformation in lake region seriously endangers water conservancy construction and the flood control capacity [5, 6].

Traditional ground leveling [7] and global positioning system (GPS) measurements cannot provide sufficient samples required by surface deformation monitoring. Interferometric synthetic aperture radar (InSAR) technology is a modern space geodetic survey technology that has developed rapidly in recent decades [8]. InSAR can not only obtain a wide range of high-precision digital elevation models (DEM) [9] but also monitor small topographic changes that range from a millimeter to meter through Differential InSAR (D-InSAR) [10]. InSAR has greatly improved its ability to monitor tiny ground deformations, especially with the development of the multitemporal (MT-InSAR) algorithm [11, 12], which overcomes temporal decorrelation and atmospheric disturbance with D-InSAR [13]. The MT-InSAR algorithm analyzes a time series of targets with high coherence points in the interferograms and then obtains the deformation velocity and cumulative deformation of the earth

surface [14]. InSAR has been successfully applied in earthquakes, landslides, and other fields [15–17].

Dongting Lake, which is the second largest freshwater lake in China, is an important regulatory and storage lake in the Yangtze River basin. Dongting Lake is a lake group composed of multiple lakes, including East Dongting Lake, South Dongting Lake, West Dongting Lake, and DaTong Lake. Dongting Lake is a wetland with a dense river network and complex biodiversity, known as "the kidney of the Yangtze River" [18]. Recently, due to the drainage silt into the East Dongting Lake area in a large amount of sediment, the river channel is continuously silted up, and the riverbed is raised [19]. The lake area continues to shrink, and the flood control efficiency is gradually weakened, which has become a threat to the ecological, economic, and social benefits of Hunan province and even the whole country [20]. Therefore, it is necessary to continuously monitor the surface deformation of the lake area to understand the process of erosion and sedimentation changes in Dongting Lake, which can qualitatively and quantitatively reflect the area, range, distribution, and dynamic changes of sediment erosion and sedimentation. This can effectively improve the scientific and effectiveness of disaster prevention flooding of Dongting Lake. However, continuous monitoring of surface deformation covering the areas of East Dongting Lake is lacking.

In this study, 84 Sentinel-1A satellite images were exploited to monitor the surface deformation of East Dongting Lake with a classical MT-InSAR algorithm, i.e., small baseline subset InSAR [12] (SBAS-InSAR). The use of SBAS-InSAR can reduce the phenomenon of temporal and spatial decoherence. However, for a study area with large surface changes such as the Dongting Lake, if the long-term deformation is directly monitored by using SBAS-InSAR, the lake areas would be basically incoherent due to the alternating process of dry and flood periods. If it is not separated for data processing, lake areas will have no results. Therefore, in this article, considering that the lake water storages in East Dongting Lake are quite different during the seasons of high and low water lines, the deformation with respect to dry and flood seasons during 2016-2019 were estimated, respectively. In addition, by processing three flood periods and three dry periods, respectively, we can compare the changes of the flood or dry seasons among different years, which were used to reflect on the intensity of surface deformation and reveal the spatial-temporal variations in the surface deformation of East Dongting Lake. Erosion and sedimentation changes in East Dongting Lake, precipitation, and human activities were considered as influencing factors, and their effects on surface deformation were studied.

2. Study Area and Datasets

2.1. Site Description. East Dongting Lake, which is located in the northeast of Hunan province, south of the Jingjiang River section of the middle reaches of the Yangtze River. The area of East Dongting Lake is 1328 km^2. The East Dongting Lake nature reserve is one of the 21 wetlands nature reserves of international importance designated by the Chinese government [21]. The specific location of East Dongting Lake is shown in Figure 1. The climate of this area is a continental subtropical monsoon humid climate. The average annual temperature is 17°C, the annual precipitation is about 1200-1300 mm, and the annual frost-free period is 285 days [22]. Dongting Lake, as one of only two river lakes in the middle and lower reaches of the Yangtze River, plays an important role in regulating the flood runoff of the Yangtze River and protecting the biodiversity of species. Previous research has indicated that the annual mean sediment is 1.7×10^9 t, of which 80% comes from the channels, 18% from the tributaries, and 2% from the local area, whereas 26% of the total sediments are transported into the Yangtze River and deposited into the lake [23]. However, due to the soil erosion in the Dongting Lake area, a large amount of sediment is discharged, the river channel is continuously silted up, and the riverbed is raised [20], which will cause surface deformation of East Dongting Lake. At the same time, there are many polders in the East Dongting Lake Plain, which is one of the state commercial grain bases. Human activities will accelerate surface fragmentation, increasing river sediment [24].

2.2. Data Used. In this study, 84 Sentinel-1A images acquired from 07 October 2016 to 10 September 2019 were collected for the study area. Sentinel-1A is a medium-high resolution C-band satellite launched by the European Space Agency (ESA) in 2014. Table 1 shows the specific parameters of Sentinel-1A used in this study. Except for resolution, another advantage is that the Sentinel-1A satellite's return cycle is only 12 days. With the launch of Sentinel-1B in 2016, a temporal resolution of 6 days could be approached. However, the Sentinel-1B data are unavailable for this study, so this study only employed Sentinel-1A data. The Sentinel-1 data are available free of charge to users around the world. In this study, considering the variation of lake water storage in East Dongting Lake during the different seasons, the time series images were divided into two groups, i.e., dry and flood seasons. It was assumed that from March to September of each year is the flood season, and that from October to February of the next year is the dry season. 12 images were selected for each one of the three dry seasons during 2017 and 2019, and 16, 18, and 14 images were selected for years 2017, 2018, and 2019, respectively. Figure 1 shows the location and geomorphology of the study area and the Sentinel-1A data coverage of part of the study area.

3. Methodology

3.1. SBAS-InSAR Processing. SBAS-InSAR inherited the advantages of the conventional D-InSAR, which generates an appropriate combination of differential interferograms produced by SAR data pairs based on the spatiotemporal baseline threshold. The interferogram satisfying the threshold condition is taken as the initial quantity, and the least square (LS) method or singular value decomposition (SVD) method is then used to obtain the average deformation rates and accumulative variables of the observation periods [24, 25].

Although SBAS-InSAR can suppress the spatiotemporal decoherence by setting the spatiotemporal baseline

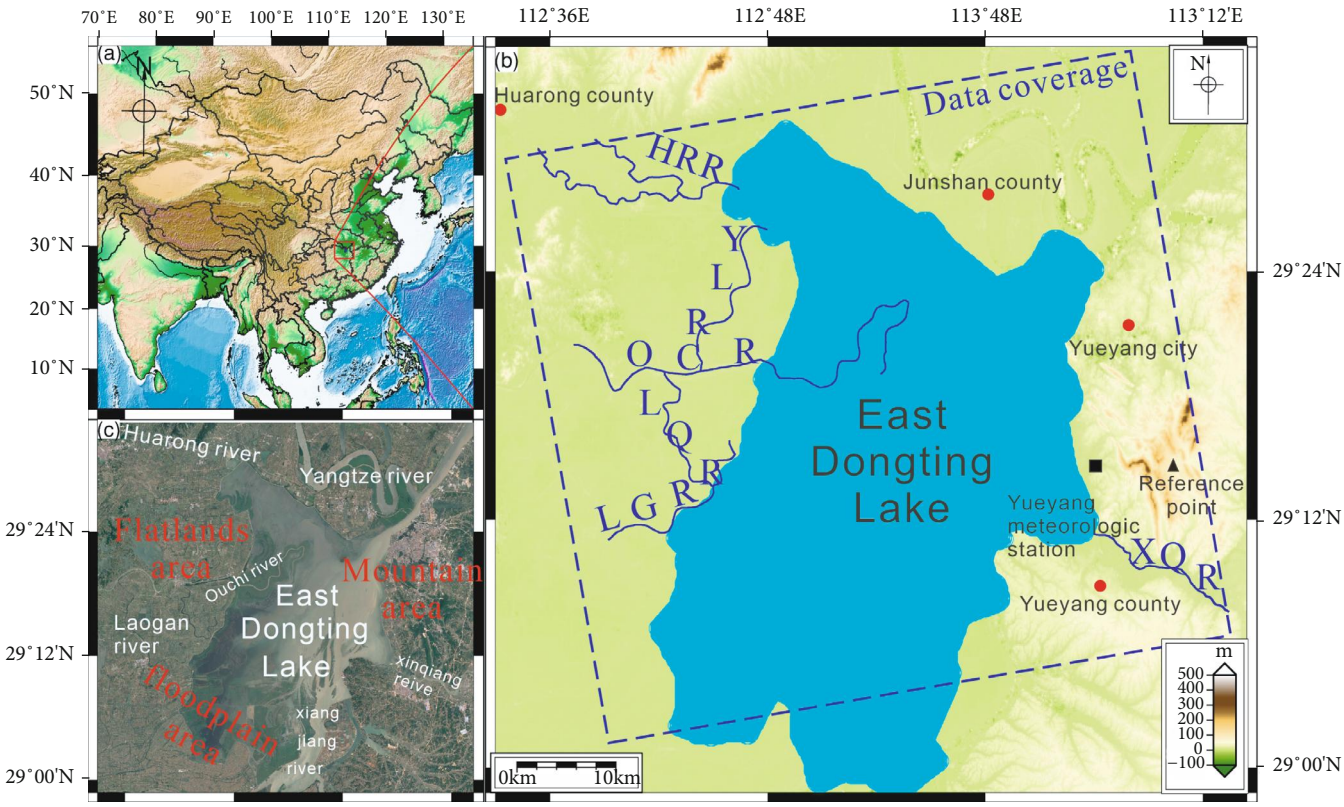

FIGURE 1: (a) Location of East Dongting Lake in China. (b) Terrain of the study area. Due to the large changes in the area of East Dongting Lake during the flood and dry periods, in this study, the embankment of the East Dongting Lake is considered as the lake boundaries, shown in light blue. Blue lines are the rivers around East Dongting Lakes. HRR: Huarong River; LQR: Longqing River; LGR: Laogan River; XQR: Xinqiang River; YLR: Yuelai River. Dark blue dashed line is the research area after subsetting of the satellite images in this paper, and red dots show the main towns. Black rectangle represents the location of the meteorological station. Black triangle represents the location of unwrapping reference point. (c) Google Earth image of East Dongting Lake acquired in flood erosion. The east is the mountainous area, the west is the flatlands, the middle south is the lake floodplain terrace, and the north is the Yangtze River floodplain.

TABLE 1: Specific parameters of Sentinel-1A data.

Parameters	Description
Product mode	Sentinel-1A IW mode
Track number	11
Azimuth angle (degree)	90
Incidence angle (degree)	43.94
Orbit direction	Ascending
Polarization	VV

thresholds, seasonal coherence decorrelation is quite serious in some specific research areas (e.g., seasonal lake areas and reservoir), where it is impossible to obtain effective interferometric pairs in the study area. Some scholars had proposed that the Intermittent Small Baseline Subset (ISBAS) method can be used to select appropriate interferometric pairs [26]. However, in this study, there are obvious dry and flood periods in East Dongting Lake. During the alternating process of dry and flood periods, the lake areas are severely incoherent. While in the flood period, this situation is even more serious. Therefore, time sequence analysis cannot be performed by combining all data.

Therefore, in this article, the SBAS-InSAR method is applied to the dataset in single season rather than the whole investigated period. At first, the data were divided into two seasons (i.e., example and flood dry periods), and then we obtained the surface deformation of each flood or dry period. There are two main points to be noted in this paper. On the one hand, flood and dry periods were classified based on the obtained images. On the other hand, the interferometric pair generated according to the spatiotemporal threshold also needs to be further selected according to the quality of the interferogram, especially in the flood season, because the temporal decorrelation is obvious.

3.2. Data Processing. All Sentinel-1A data were registered to the same common master image of each period. The acquisition data of the super master image for the dry and flood seasons selected in this study were December 30, 2016; June 4, 2017; December 13, 2017; May 6, 2018; December 20, 2018; and June 18, 2019, respectively. In order to avoid the phase jump phenomenon caused by different bursts with Terrain Observation by Progressive scans SAR (TOPSAR) modes of Sentinel-1A data, Shuttle Radar Topography Mission (SRTM) DEM data provided by National Aeronautics and Space Administration (NASA) were used for assistant

registration in this study. As mentioned above, the ground coverage corresponding to the Sentinel-1A image is 250 km × 250 km. In order to reduce the unnecessary data and calculation, the data located outside the research area were removed in this experiment.

In order to reduce the phase noise, 10 × 2 (range × azimuth) multilook rate was adopted in data processing. In the differential process, 30 m SRTM data were used as external DEM data to remove the topographic phase. In order to avoid the generation of small isolated baselines and maintain the requirement of coherence, the threshold of the perpendicular baseline was 80 m. In addition, decorrelation will also occur when the time interval between two images is too long, which will affect the final accuracy. Therefore, the threshold of the temporal baseline was set as 60 days for both the dry and flood period. The temporal and perpendicular baselines of the used interferograms are shown in Figure 2.

The interferograms were generated according to the small baseline set image pairs selected [26]. In order to improve the quality of the interferogram, the spatial adaptive filtering method was used to eliminate random noise in the interferogram [27]. Then, phase unwrapping of the interferogram was carried out with the minimum cost flow method. In this method, a stable point in the research period is required as the start point of unwrapping. Phase unwrapping was conducted by choosing a pixel located in Yueyang city as a reference point. The location of the reference point is shown as a black triangle in Figure 1(b).

According to the coherence value, the interferograms with a relatively high coherence were selected as the unwrapping mask of the flood and dry season data, and the average coherence threshold in dry and flood seasons was 0.5 and 0.3, respectively. According to the characteristics of the lake water line in the flood and dry periods, different unwrapping masks should be determined in advance, according to the coherence of differential interferograms before phase unwrapping. Meanwhile, interferometric pairs with low coherence and poor unwrapping were removed. Finally, we obtained 41, 32, and 32 differential interferograms in the dry season of 2017, 2018, and 2019, respectively, and 47, 64, and 40 differential interferograms in the flood season of 2017, 2018, and 2019, respectively. Figure 3 shows the representative differential interferograms for each season. Moreover, the differential phase includes the elevation residual phase, atmospheric delay phase, and noise phase. Therefore, it is necessary to remove other phases to obtain an accurate deformation [12]. In order to reduce the error caused by low coherence in the differential interferograms, the SBAS-InSAR algorithm only calculates the high coherence points. In this study, the coherence coefficient average threshold method was used to select high coherence points [28, 29].

4. Results

4.1. Mean Rate in the Dry Season. Figure 4 shows the monthly average surface deformation rate the of the study area, during the dry season. The map is superimposed on the Google Earth image of East Dongting Lake acquired in each dry season, and the white line is the embankment of East Dongting Lake. Positive values represent that the surface is getting closer to the radar along the line of sight (LOS) direction, and negative value surface is further away from the radar in the LOS direction. The water line of East Dongting Lake started to rise at the beginning of the annual flood season and then reached the peak at the end of July and early August. After that time, Chenglingji (one of the East Dongting Lake outlets) began to open floodgates to reduce the volume of East Dongting Lake water. Subsequently, in the dry season, the lake area began to decrease, and the running water carried away the lake silt in the area, causing surface settlement in the lake floodplain.

Region A is in the floodplain area at the south-central side of East Dongting Lake, and the main settlement is distributed along the inner channel with an average deformation velocity of about -3 mm/month in 2017. In the 2018 dry season, the intensity of deformation was even greater around the region, and the average rate of the settlement reached -6 mm/month. The settlement in this area mainly occurs on the southern floodplain terraces and on both banks of the rivers inside the lake. The main cause is the river water entering the lake during the dry season and the internal water flow of the lake scouring the surrounding soil. In the 2019 dry season, the average rate decreased to about -2 mm/month. There is another channel along the embankment in the southwest. During the dry season, there is also flowing water to flow through the surrounding silt, which could cause the settlement center moved southwest in 2019.

Region B is located at the entrance of Xinqiang River in the east of East Dongting Lake, and the river twists and turns in the region. The average rates of settlement in 2017 and 2018 were about -5 and -6 mm/month, respectively. There are two reasons for this settlement. First, the river has twists and turns, making it easier for sediment to accumulate in the water during the flood period. When the sediment is not completely integrated into the lake surface during the dry period, it is more likely to be eroded. Second, the flowing water outside Xinqiang River will directly scour this area. However, surface deformation was hardly observed in this region in the 2019 dry season. This can be ascribed to the gentle water flow of this tributary and Xinqiang River caused by the relatively less precipitation in the previous year (i.e., 2018). In addition to the deformation at the entrance of the Xinqiang River, the deformation is found in the entrance of the Ouchi River.

Region C (see Figure 4(b)) is a small area of surface settlement in the northwest corner of East Dongting Lake, where there is a small reservoir. If the water line of East Dongting Lake is too high to threaten other areas, this reservoir can regulate and store East Dongting Lake for water storage and begin to drain outwards in the dry period. In the reservoir, an obvious settlement velocity of about -5 mm/month was only detected in 2018. It is reported that there was a serious flooding disaster in East Dongting Lake in the summer of 2017, which caused the increase of silt in the entire lake area [30]. This small reservoir also contained a large amount of mud and soil. Therefore, when the water level drops during the dry season of the next year (i.e., 2018), the drainage

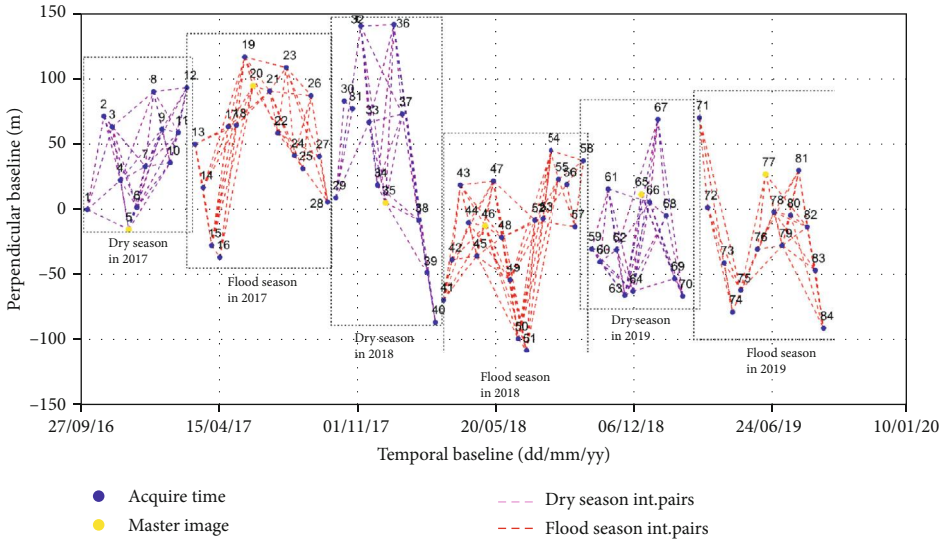

Figure 2: Temporal and perpendicular baselines of study periods. Blue dots represent the image acquisitions, and yellow dots represent the super master images. Purple and red dashed lines represent interferometric pairs with the dry and flood seasons, respectively.

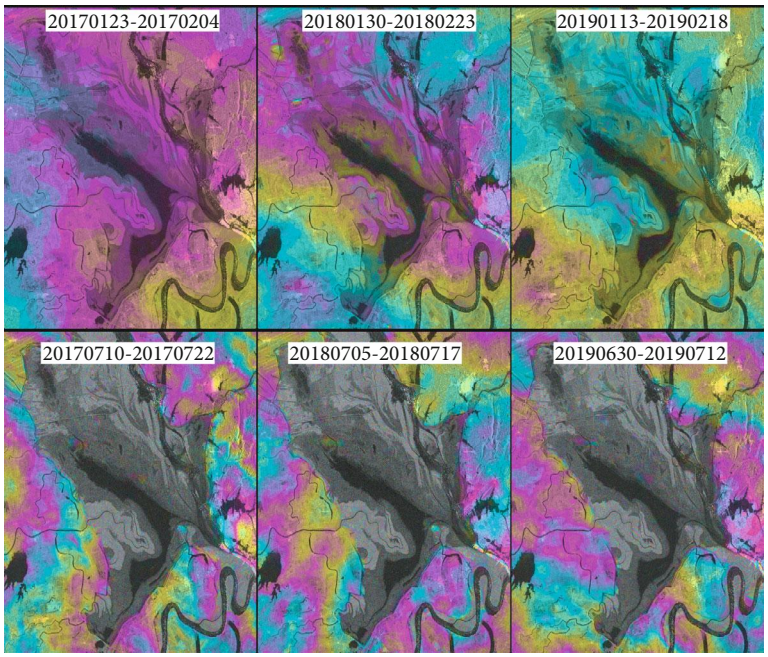

Figure 3: Representative differential interferograms for each season, the first row is the differential interferogram in the dry period, and the second row is the differential interferogram in the flood period. Acquired time of differential interferogram is presented at the top of each subplot.

process will wash out the coastal soft soil, leading to coastal erosion and collapse.

Trends in the East Dongting Lake surface deformation intensity grade dynamic changes in time and space could be indicated by analyzing the settlement and sedimentation grade in East Dongting Lake with dry season. We use a method similar to the equidistant division to divide the deformation rate. The purpose of this division is to assess the degree of surface deformation of the East Dongting Lake in comparison with the water regime. The deformation intensity are divided into six classes, including a severe settlement area (<-4 mm/month), moderate settlement area (-4 to -2 mm/month), slight settlement area (-2 to -0.5 mm/month), stable area (-0.5 to 0.5 mm/month), slight sedimentation area (0.5 to 2 mm/month), and severe sedimentation area (>2 mm/month). The areas of each surface deformation intensity grade of dry seasons are compared in Table 2.

In the dry season, the severe settlement area, moderate settlement area, slight sedimentation area, and severe sedimentation area all experienced the change of increasing from 2017 to 2018 and then decreasing from 2018 to 2019. On the

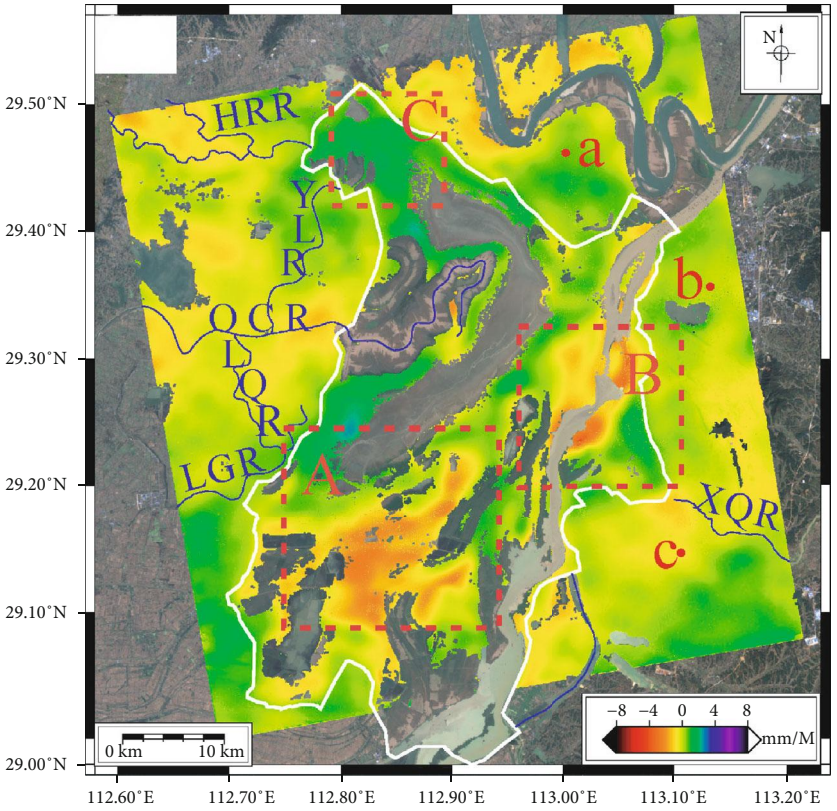

(a)

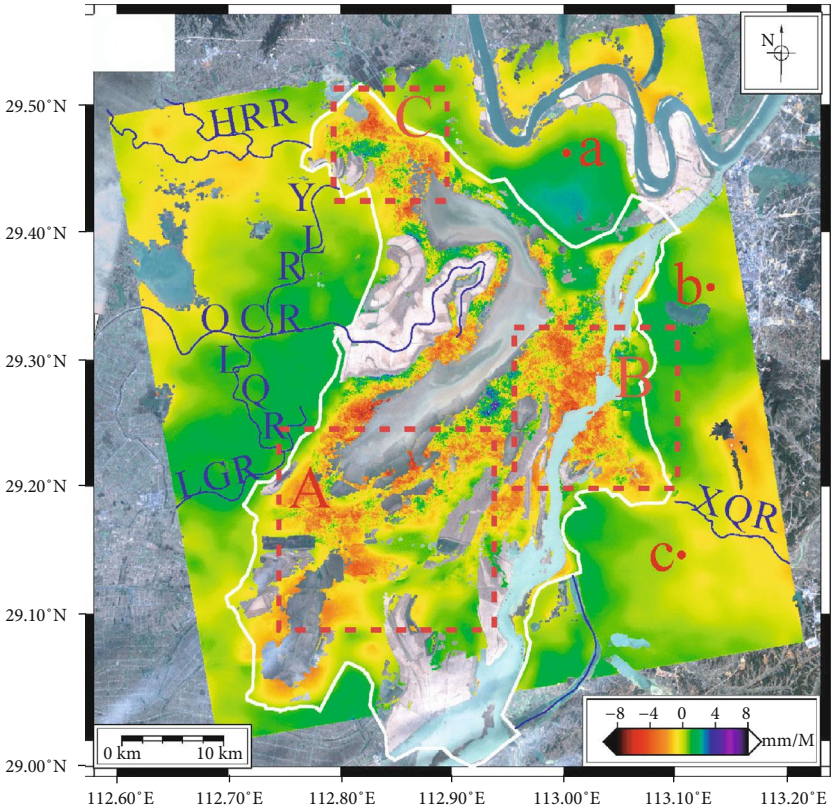

(b)

Figure 4: Continued.

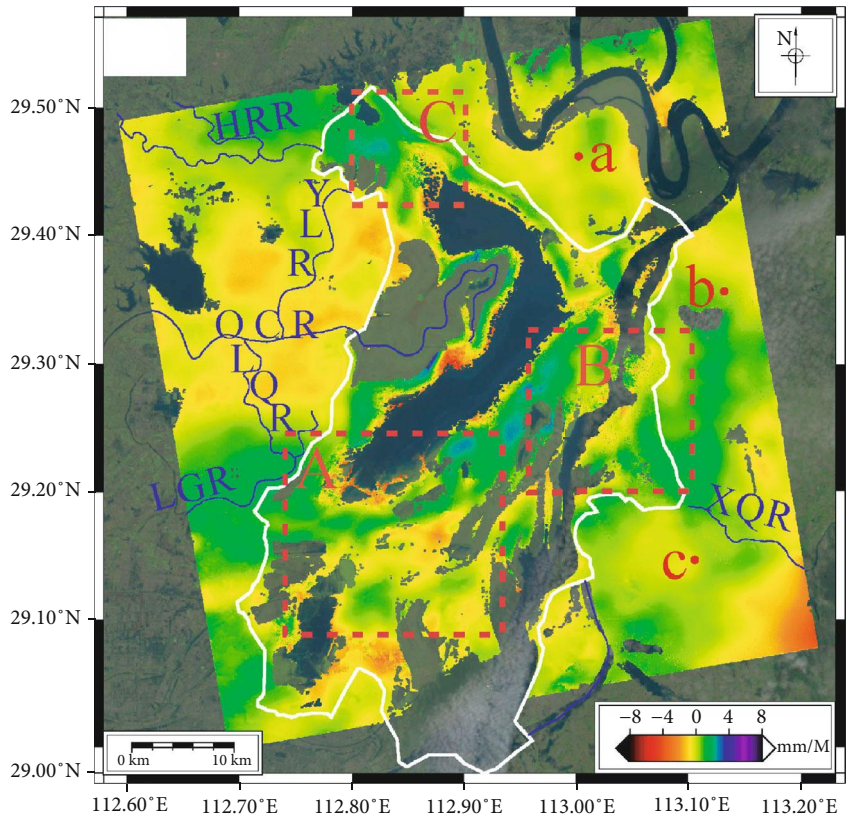

(c)

Figure 4: The monthly average deformation rate along LOS direction across East Dongting Lake during the dry season of 2017 (a), 2018 (b), and 2019 (c). The base image is an optical image of each dry season. White line represents the embankment of East Dongting Lake, and the blue lines are the rivers around East Dongting Lakes. HRR: Huarong River; LQR: Longqing River; LGR: Laogan River; XQR: Xinqiang River; YLR: Yuelai River. Red dots represent the main towns. a: Junshan district, b: Yueyang city, and c: Yueyang county. Region A: southern floodplain area, Region B: entrance of the Xinqiang River, and Region C: northwest catchment area.

Table 2: Comparison of the intensity grades of surface deformation in the dry seasons.

Intensity grade of surface deformation	Surface deformation area in the dry season					
	2017		2018		2019	
	Area (km^2)	%	Area (km^2)	%	Area (km^2)	%
Severe settlement	0.04	0.002	6.62	0.370	0.88	0.050
Moderate settlement	19.99	1.121	67.68	3.781	15.82	0.895
Slight settlement	356.10	19.968	349.78	19.542	335.50	18.985
Stable area	959.70	53.814	717.26	40.072	843.28	47.720
Slight sedimentation	440.93	24.725	619.87	34.631	549.04	31.069
Severe sedimentation	6.59	0.370	28.70	1.604	22.64	1.281

contrary, the areas of slight settlement and stable area experienced a decrease followed by an increase during the three years' dry seasons. According to the deformation areas presented in Table 2, it can be found that the deformation intensity was 2018 > 2019 > 2017 for the dry season. Comparing the changes in the area of sedimentation and settlement, we can find that the sedimentation and settlement in East Dongting Lake are synergistic and simultaneous. Meanwhile, the stable areas still account for at least 40% of areas for the dry season. These stable areas are mainly located in the outer areas of East Dongting Lake.

4.2. Mean Rate in the Flood Season. The water level of East Dongting Lake rises during the flood season. Due to the specular reflection on the water surface, the echo signal is weak, and even local areas have no coherence. Therefore, there are no coherence points inside East Dongting Lake. As a result, surface deformation in the flood season can only be obtained by analyzing the deformation around East Dongting Lake basin. Flood runoff will scour away loose surface soil along slopes and river valleys and cause river silt. Moreover, in the flood season, the water flow is large and the flow velocity is fast, exhibiting great transportation and scour ability.

This means that the flood not only carries the sediment carried by the storm runoff but also scours the riverbed and riverbank, bringing the original sediment from the river valley into the turbulent flow and East Dongting Lake.

During the flood season, the tributary water system of East Dongting Lake plays an important role in the process of surface deformation. The first is Huarong River basin, which is on the northwest of East Dongting Lake; the second is the Ouchi River basin, which include three tributaries, i.e., Laogan River, Longqing River, and Yuelai River; the third is the basin of Xinqiang River on the eastern of East Dongting Lake; and the last is the sandbank in the southeast of East Dongting Lake. Figure 4 shows the surface deformation of East Dongting Lake in each flood season.

Region D shows the surface deformation of the Huarong River Basin, which is located in the northwest of East Dongting Lake, and is one of the "four mouths" of the Yangtze River flowing into East Dongting Lake, which has played an important role in regulating the flood season of the Yangtze River. There was obvious settlement area mainly concentrated in the northern part of Huarong River during the flood season in 2017 and 2019. The settlement rate in 2017 was about -3 mm/month. In 2019, settling velocity phenomenon was more serious, with the value exceeding -4 mm/month. There was no obvious settlement around the Huarong River in 2018, which can be ascribed to a relatively smaller Yangtze River flood run-off in 2018, as indicated by the relatively less precipitation in 2018. Region E is the surface deformation area around Ouchi River and its three tributaries. Ouchi River is located in the west of East Dongting Lake. It is also one of the "four mouths" of the Yangtze River flowing to East Dongting Lake. Compared with the Huarong River, the Ouchi River is longer and has a wider basin and more tributaries. During the flood season in 2017, there was obvious surface settlement around the Laogan River and Longqing River, with the settlement rate being about -3 mm/month. In 2018, the areas with settlement center were mainly concentrated in the west of the Yuelai River, and the rate was also nearly -3 mm/month. In the 2019 flood season, there was a relatively serious settlement area in south of Laogan River and Longqing River, with a velocity of about -6 mm/month. This is mainly an agricultural planting area, where irrigation water will accelerate the flow of water and have a stronger scouring effect on the surrounding area. In addition, human activities in agricultural areas may also loosen the surface soil and be more easily washed by running water.

The Xinqiang River located in Region F is an important river for the East Dongting Lake Basin. During the flood season, floods in the eastern mountainous areas flow through the Xinqiang River into the East Dongting Lake. In Figure 5, we found that the settlement phenomenon became more and more serious in the Xinqiang River Basin from 2017 to 2019. In 2019, the rate of settlement reaches up to -4 mm/month. In 2017 and 2018, the maximum deformation settlement rates were close to -2 mm/month. However, the surface settlement area was larger in 2017 than that in 2018. We can find that there are more serious erosion gullies in the floodplain of Xinqiang River watershed.

In addition to the three main drainage networks mentioned above, there was also a perennial settlement area in the sandbank at the southeast of East Dongting Lake (see Region G in Figure 5). The surface deformation rate of this area is up to about -4 mm/month. Besides, this region is basically a rice planting area with agricultural planting and human activity; therefore, the surface deformation can be related to the Laogan River area as well as irrigation and agricultural activities.

As shown in Table 3, the intensity grades of surface deformation are also classified during the flood season. The severe settlement area, moderate settlement area, slight settlement area, slight sedimentation area, and severe sedimentation area all experienced the change of first decreasing and then increasing from 2017 to 2019, and the stable areas experienced a decrease followed by an increase during flood seasons. By comparing the area of surface deformation, it could be found that the deformation intensity was 2017 > 2019 > 2018 for the flood season. We also noticed that, before the flood season of 2018, East Dongting Lake experienced the most serious subsidence phenomenon in the 2018 dry season. This indicates that after having experienced strong settlement and sedimentation, the earth surface in East Dongting Lake maintains a period of relative stability. Therefore, we found that, during the 2018 flood season, the stable area accounted for 56.994%, and slight settlement and slight sedimentation accounted for 21.282% and 21.061%, respectively. Those three deformation intensity grade areas dominated more than 99% of the observed area.

4.3. Time Series Deformation of East Dongting Lake. Although the method proposed in this study can obtain the results of surface deformation in different periods, the time series deformation of the study period cannot be proved. In this section, we use the conventional SBAS-InSAR method to combine all images to obtain the time series of the surface deformation.

Figure 6 shows the average deformation rate during the whole investigated period and the time series deformation of the feature points.

As shown in Figure 6(a), the deformation area obtained from the whole investigated period is similar to that obtained from the flood season. It can be found that the deformation area is located at the external river network of East Dongting Lake (e.g., Huarong River, Ouchi River, Xinqiang River, and Langan River). The average rate of deformation during the whole investigated period is smaller than those during the dry or flood seasons. This can be ascribed that the sedimentation and the settlement effects in the dry and flood seasons offset each other in the long-term deformation results. In order to show more details of the detected surface deformation, the time series deformations over the three typical feature points located at the external river network are shown in Figure 6(b). It was found that the selected three feature points basically showed a linear settlement during the dry period. However, the time series deformation shows obvious fluctuations during the flood period, which is highly correlated to the precipitation increase at the same time. This also demonstrates that the precipitation in the flood season

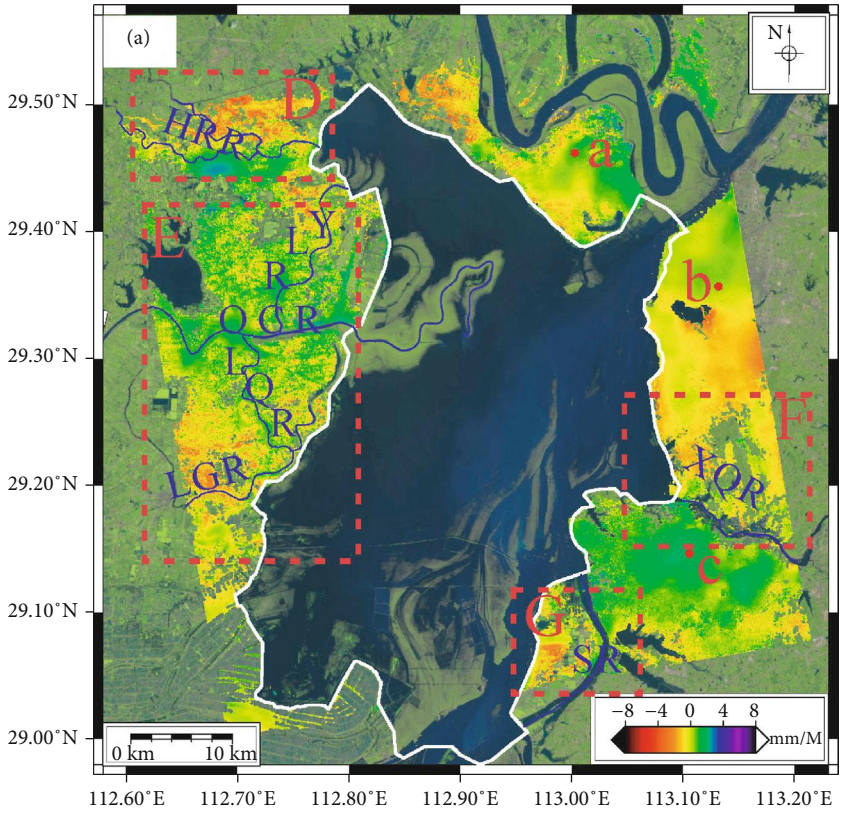

(a)

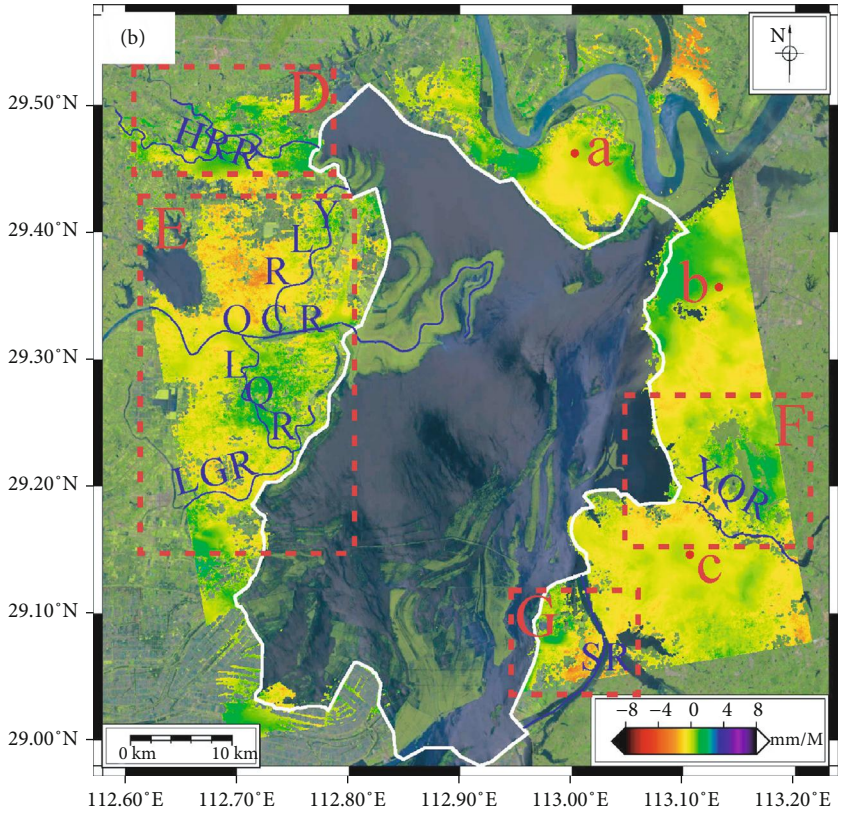

(b)

Figure 5: Continued.

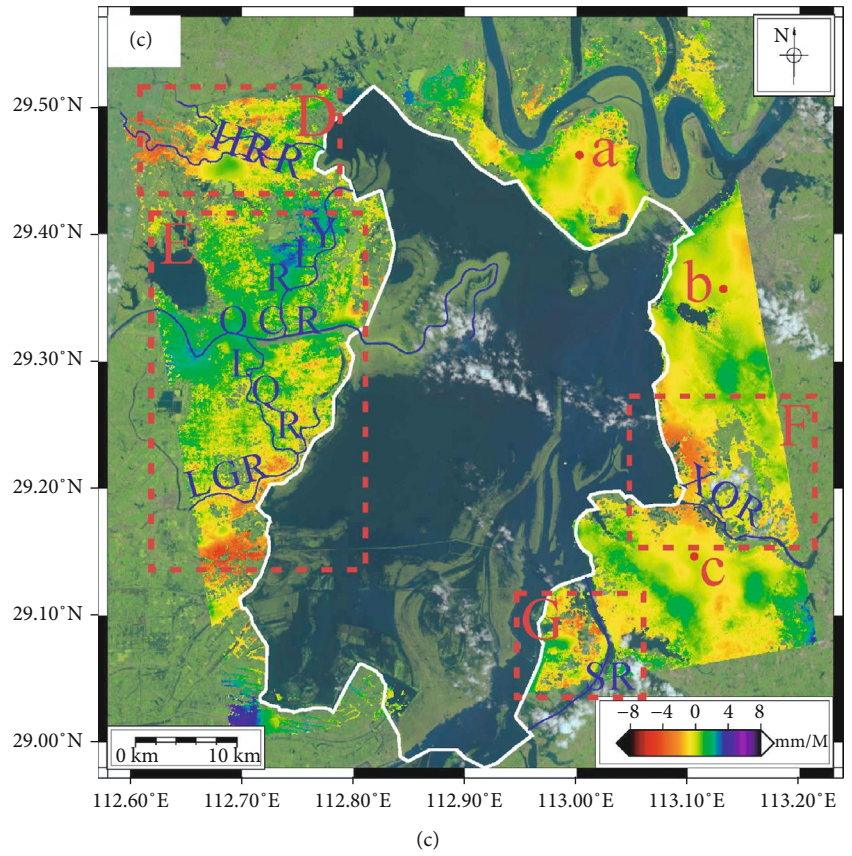

Figure 5: Surface deformation rate caused by soil erosion in East Dongting Lake during the flood season of 2017 (a), 2018 (b), and 2019 (c). The base image is an optical image of each flood season. The white line represents the embankment of East Dongting Lake, and the blue lines are the rivers around East Dongting Lake. HRR: Huarong River; LQR: Longqing River; LGR: Laogan River; XQR: Xinqiang River; SR: sandbank area; YLR: Yuelai River. Region D: Huarong River Basin, Region E: Ouchi River and its tributaries, Region F: Xinqiang River Basin, and Region G: sandbank area. Red dots represent the main towns. a: Junshan district, b: Yueyang city, and c: Yueyang county.

Table 3: Comparison of the intensity grades of surface deformation in the flood seasons.

Intensity grade of surface deformation	Surface deformation area in the flood season					
	2017		2018		2019	
	Area (km^2)	%	Area (km^2)	%	Area (km^2)	%
Severe settlement	0.16	0.019	0	0	3.11	0.352
Moderate settlement	20.75	2.493	4.85	0.550	32.80	3.717
Slight settlement	211.37	25.396	187.88	21.282	200.53	22.727
Stable area	309.07	37.135	503.14	56.994	348.10	39.451
Slight sedimentation	277.50	31.805	185.93	21.061	257.34	29.165
Severe sedimentation	13.44	1.802	1.00	0.113	40.49	4.588

dominates the surface deformation in the East Dongting Lake area.

5. Discussion

5.1. Influence of Precipitation on Surface Deformation. Figure 7 shows the daily precipitation and deformation intensity grade percent during the study period. In Figure 7, it is observed that the number of days with precipitation in the flood season is more than that in the dry season. We discovered that, in the flood season, the surface settlement is positively correlated with precipitation events, indicating that deformation may be caused by flood events after heavy precipitation. Since the precipitation cannot infiltrate in time, a large amount of sediment is mixed with running water and promoted the erosion of surrounding river embankments. While in the dry season, the deformation is negatively correlated with precipitation events. Previous studies have pointed out that a small amount of precipitation will increase the soil viscosity, thereby playing a role in inhibiting soil erosion [31]. In the dry season, with less precipitation and weak intensity, after the tiny sediment particles are wetted by

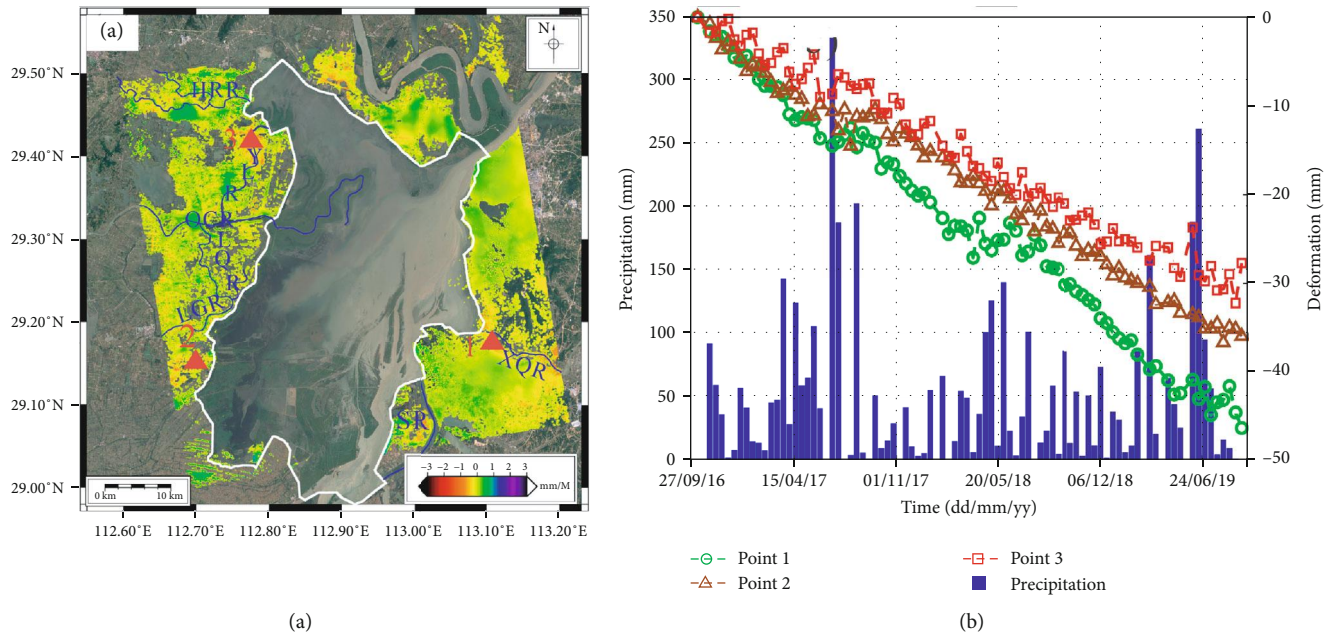

Figure 6: (a) Deformation rate obtained from the whole investigated period. White line represents the embankment of East Dongting Lake, and the blue lines are the rivers around East Dongting Lakes. HRR: Huarong River; LQR: Longqing River; LGR: Laogan River; XQR: Xinqiang River; YLR: Yuelai River; SR: sandbank area. Red triangles represent the feature points. (b) Time series deformations of the points of interest and the precipitation during the whole investigated period.

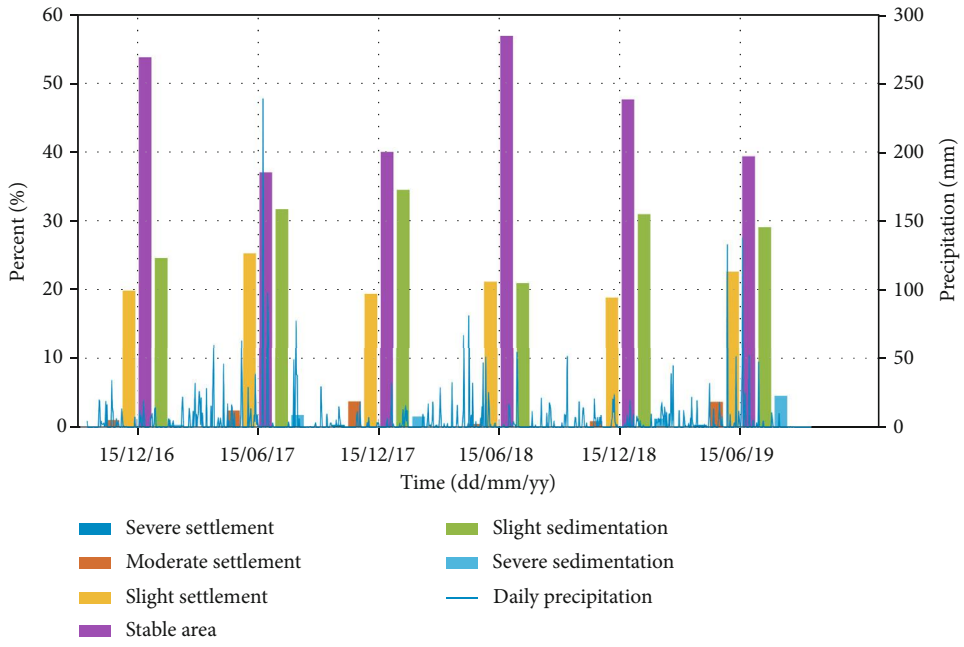

Figure 7: Daily precipitation and surface deformation intensity during the study period.

precipitation, the upper soil can more easily adhere to the surface with particles, and the cohesion is stronger.

Generally, the area is more stable in the dry season than the flood season, as the results in 2017 and 2019. However, there is an abnormal phenomenon in 2018, and the percent of the stable area is larger in the dry season than in the flood season. This is somewhat expected since the precipitation days and the maximum precipitation during the flood season in 2018 were both smaller than in 2017 and 2019. The precipitation and the number of precipitations during the dry season in 2018 were also smaller than in 2017 and 2019. The less precipitation in the dry season, the more obvious the deformation phenomenon [32]. Therefore, the surface deformation during the dry season in 2018 is the most obvious. Another reason is that during the flood season in 2017, there was a catastrophic flood disaster event in the Dongting Lake

area. This disaster event showed that a lot of silt and sediment remained in East Dongting Lake [30]. Therefore, during the dry season, the settlement of the soil occurred on the surface.

5.2. Causes of Surface Deformation in East Dongting Lake

5.2.1. Soil Erosion. As a geomorphic process persistently occurring over the earth's surface, soil erosion is one of the most serious environmental problems in the world nowadays, seriously threatening agriculture, soil nutrients, and surface integrity [33]. The wetland of Dongting Lake Plain is a key prevention zone for soil erosion in Hunan Province. Dongting Lake undertakes the sediment of major rivers in Hunan Province, and the soil erosion modulus of the basin is about 3970 t/km^2 [34]. The main type of soil erosion is water erosion, including surface erosion and gully erosion. There are also a small amount of soil erosions such as collapse and landslides in local areas. The flood season is the key sedimentation period of East Dongting Lake, and the deposited sediment exceeds the annual average sediment sedimentation. However, in the dry season, the erosion effect is greater than the sedimentation effect, and 10% of the sedimentation amount in the flood season are washed out of East Dongting Lake [35]. In addition, the sedimentation during the flood season indicates that soil erosion and transportation in the eastern mountainous area and western plain area are mainly related to storm runoff and flood runoff. The surface deformation monitored in this study shows in good agreement with the soil erosion feature. Therefore, we can speculate that soil erosion and siltation are the main reason for the surface deformation of East Dongting Lake.

The lake water contains a lot of sediment during the flood season, and in the dry season, the water line of the lake then drops, so the remaining sediment on the floodplain will flow into the catchment area with the flowing water and may erode the flowing area. Especially at the junction of the floodplain and the catchment area, the erosion effect becomes more obvious under the dual action of external flowing water and catchment water circulation. Settlement in East Dongting Lake area is mainly centralized in the south and west of the catchment, which indicates that the erosion in those areas is very significant. These two catchments are the main source of water flow in the dry season. Another settlement region is in the middle of the eastern part of East Dongting Lake. When the flowing water passes through the bend in the dry season, the pressure of the flowing water increases, the river water exerts a greater erosion force on the river bank, and the erosion effect is more obvious.

During the flood season, all the surface settlement regions are distributed in East Dongting Lake of the main external drainage. There are two main sources of river flooding. The first is the flooding of Yangtze River, which mainly occurs in the Ouchi River and its tributaries and Huarong River in the west of East Dongting Lake. There are also floods caused by the eruption of mountain torrents during the flood season in the eastern mountainous area, which mainly flow through the Xinqiang River area. Among them, only Xinqiang River and Laogan River keep a state of continuous erosion, and the erosion velocity is gradually increasing, indicating that surface settlement in the basin is getting more and more serious. In addition, according to the Yangtze River Sediment Loss Bulletin, the sediment flow in East Dongting Lake in 2018 was less than that in other years [36], which agreed with the results of this study.

The soil erosion of East Dongting Lake has the following characteristics based on the above analysis. First, the surface soil has been eroded and sedimentation both in the flood and dry periods. Second, in the dry season, erosion and sedimentation mainly occur in the internal river channels and catchment of the lake, and in the flood season, erosion mainly occurs in the area where the river flows. Third, flood disasters in flood season will have an impact on erosion and sedimentation in the later dry season.

5.2.2. Human Activities. In addition to soil erosion, human activities could be another reason for surface deformation. It had been found that human activities would affect the hydrological conditions of lakes [37]. Moreover, agricultural reclamation will cause soil destruction in the reclamation area, which is more susceptible to erosion, and increases in sediments in the river [38]. There are many polders in the East Dongting Lake Plain, which is one of the state commercial grain bases. Human activities and irrigation water extraction in the process of agricultural planting can also cause surface deformation in some areas. As expected, this part of the deformation is mainly concentrated in the agricultural planting stage, which corresponds to the flood period in this study. In addition, the study area also includes some urban areas. The rapid urbanization process, infrastructure construction, groundwater extraction, or other urban development processes may cause regional surface deformation. As shown in Figures 4 and 5, it is found that there are some small deformation areas in the urban area.

6. Conclusion

East Dongting Lake area is selected as the area of deformation monitoring with InSAR. It is found that the unique lake morphology of Dongting Lake, i.e., "river facies in dry period, lake facies in flood period," has a greater impact on the coherence. If the SBAS-InSAR method is used to the multi-years of dataset, serious errors will be caused in the subsequent deformation result estimation. Therefore, the Sentinel-1A data acquired on the East Dongting Lake are divided into different groups according to dry and flood seasons. Surface deformations are estimated for the flood and dry seasons, respectively.

The results show that during the dry season of Dongting Lake, the surface deformation was the most serious in 2018. Almost the entire lake area had settlement and sedimentation. The flood disasters in 2017 and 2019 were relatively slight, so the surface deformation areas are mainly concentrated around the already catchment areas along the rivers in the lake. During the flood season, we found that the most severe surface deformation occurred in 2017, indicating that the flood disaster not only had a serious impact on the

surface deformation inside the lake but also had an impact on the drainage network outside the East Dongting Lake.

Through the analysis of the deformation feature and precipitation, it is believed that the surface deformation detected by the SBAS-InSAR method is basically caused by lake mud erosion and sedimentation. Therefore, InSAR could be a potential method for the monitoring of soil erosion. Compared with the current methods [39, 40], SBAS-InSAR can provide quantitative results of soil erosion with high spatial resolution and avoid the time-consuming and laborious problem of manual verification in the general model.

Data Availability

Copernicus Sentinel data 2016-2019 processed by the European Space Agency (ESA) were retrieved from the ASF Distributed Active Archive Center (DAAC) (https://search.asf.alaska.edu/#/). The precipitation data are provided by the China Meteorological Data Service Center (http://data.cma.cn).

Conflicts of Interest

The authors declare no conflicts of interest.

Acknowledgments

Copernicus Sentinel data 2016-2019 processed by the European Space Agency (ESA) were retrieved from the ASF Distributed Active Archive Center (DAAC) (https://vertex.daac.asf.alaska.edu/#). The precipitation data are provided by the China Meteorological Data Service Center (http://data.cma.cn). This study was supported by the National Natural Science Foundation of China (Nos. 41704001 and 42030112), the Hunan Natural Science Foundation (Nos. 2020JJ2043 and 2018JJ3347), the Special funds for the construction of Hunan innovative province (No. 2019GK5006), and the Project of Innovation-driven Plan of Central South University (No. 2019CX007).

References

[1] M. R. Rahman, Z. H. Shi, and C. Chongfa, "Soil erosion hazard evaluation—an integrated use of remote sensing, GIS and statistical approaches with biophysical parameters towards management strategies," *Ecological Modelling*, vol. 220, no. 13-14, pp. 1724–1734, 2009.

[2] Y. Gao, Z. Liang, B. Wang, Y. Wu, and P. Wu, "Wetland change detection using cross-fused-based and normalized difference index analysis on multitemporal Landsat 8 OLI," *Journal of Sensors*, vol. 2018, Article ID 8130470, 8 pages, 2018.

[3] W. H. McAnally, C. Friedrichs, D. Hamilton et al., "Management of fluid mud in estuaries, bays, and lakes. I: present state of understanding on character and behavior," *Journal of Hydraulic Engineering ASCE*, vol. 133, no. 1, pp. 9–22, 2007.

[4] L. G. Zheng, G. J. Liu, Y. Kang, and R. K. Yang, "Some potential hazardous trace elements contamination and their ecological risk in sediments of western Chaohu Lake, China," *Environmental Monitoring and Assessment*, vol. 166, no. 1-4, pp. 379–386, 2010.

[5] D. Fan, C. Li, D. Wang, P. Wang, A. W. Archer, and S. F. Greb, "Morphology and sedimentation on open-coast intertidal flats of the Changjiang Delta, China," *Journal of Coastal Research*, vol. 43, pp. 23–35, 2004.

[6] F. Xu, J. Tao, Z. Zhou, G. Coco, and C. Zhang, "Mechanisms underlying the regional morphological differences between the northern and southern radial sand ridges along the Jiangsu Coast, China," *Marine Geology*, vol. 371, pp. 1–17, 2016.

[7] G. Desir, F. Gutiérrez, J. Merino et al., "Rapid subsidence in damaging sinkholes: measurement by high-precision leveling and the role of salt dissolution," *Geomorphology*, vol. 303, pp. 393–409, 2018.

[8] K. Yang, L. Yan, G. Huang, C. Chen, and Z. Wu, "Monitoring building deformation with InSAR: experiments and validation," *Sensors*, vol. 16, no. 12, p. 2182, 2016.

[9] H. A. Zebker and R. M. Goldstein, "Topographic mapping from interferometric synthetic aperture radar observations," *Journal of Geophysical Research*, vol. 91, no. B5, pp. 4993–4999, 1986.

[10] A. K. Gabriel, R. M. Goldstein, and H. A. Zebker, "Mapping small elevation changes over large areas: differential radar interferometry," *Journal of Geophysical Research*, vol. 94, no. B7, pp. 9183–9191, 1989.

[11] A. Ferretti, C. Prati, and F. Rocca, "Permanent scatterers in SAR interferometry," *IEEE Transactions on Geoscience and Remote Sensing*, vol. 39, no. 1, pp. 8–20, 2001.

[12] P. Berardino, G. Fornaro, R. Lanari, and E. Sansosti, "A new algorithm for surface deformation monitoring based on small baseline differential SAR interferograms," *IEEE Transactions on Geoscience and Remote Sensing*, vol. 40, no. 11, pp. 2375–2383, 2002.

[13] J. Dong, L. Zhang, M. S. Liao, and J. Y. Gong, "Improved correction of seasonal tropospheric delay in InSAR observations for landslide deformation monitoring," *Remote Sensing of Environment*, vol. 233, p. 111370, 2019.

[14] C. H. Lu, C. F. Ni, C. P. Chang, J. Y. Yen, and R. Y. Chuang, "Coherence difference analysis of sentinel-1 SAR interferogram to identify earthquake-induced disasters in urban areas," *Remote Sensing*, vol. 10, no. 8, p. 1318, 2018.

[15] X. Yu, J. Hu, and Q. Sun, "Estimating actual 2D ground deformations induced by underground activities with cross-heading InSAR measurements," *Journal of Sensors*, vol. 2017, Article ID 3170506, 12 pages, 2017.

[16] B. Hu, B. Yang, X. Zhang, X. Chen, and Y. Wu, "Time-series displacement of land subsidence in Fuzhou downtown, monitored by SBAS-InSAR technique," *Journal of Sensors*, vol. 2019, Article ID 3162652, 12 pages, 2019.

[17] M. Tzouvaras, C. Danezis, and D. G. Hadjimitsis, "Small scale landslide detection using sentinel-1 interferometric SAR coherence," *Remote Sensing*, vol. 12, no. 10, p. 1560, 2020.

[18] Y. Tang, Y. H. Xie, F. Li, and X. S. Chen, "Spatial distribution of emergent herbaceous wetlands in the East Dongting Lake during the last twenty years based landsat data," *Resources and Environment in the Yangtze Basin*, vol. 22, pp. 1484–1492, 2013.

[19] B. F. Wu, J. L. Huang, and L. B. Shen, "Analysis and evaluation of flood-control functions of wetland taking Dongting Lake as an example," *Geographical Research*, vol. 19, pp. 189–193, 2000.

[20] J. Li, H. Yin, J. Chang, C. Lu, and H. Zhou, "Sedimentation effects of the Dongting Lake area," *Journal of Geographical Sciences*, vol. 19, no. 3, pp. 287–298, 2009.

[21] Y. Yuan, G. Zeng, J. Liang et al., "Effects of landscape structure, habitat and human disturbance on birds: a case study in East Dongting Lake wetland," *Ecological Engineering*, vol. 67, pp. 67–75, 2014.

[22] C. Hu, Z. M. Deng, Y. H. Xie, X. S. Chen, and F. Li, "The risk assessment of sediment heavy metal pollution in the East Dongting Lake Wetland," *Journal of Chemistry*, vol. 2015, Article ID 835487, 8 pages, 2015.

[23] G. Jun-Feng, Z. Chen, J. Jia-Hu, and H. Qun, "Analysis of deposition and erosion of Dongting Lake by GIS," *Journal of Geographical Sciences*, vol. 11, no. 4, pp. 402–410, 2001.

[24] A. Hooper, "A multi-temporal InSAR method incorporating both persistent scatterer and small baseline approaches," *Geophysical Research Letters*, vol. 30, article L16302, 2008.

[25] F. Casu, M. Manzo, and R. Lanari, "A quantitative assessment of the SBAS algorithm performance for surface deformation retrieval from DInSAR data," *Remote Sensing of Environment*, vol. 102, no. 3-4, pp. 195–210, 2006.

[26] A. Sowter, L. Bateson, P. Strange, K. Ambrose, and M. F. Syafiudin, "DInSAR estimation of land motion using intermittent coherence with application to the South Derbyshire and Leicestershire coalfields," *Remote Sensing Letters*, vol. 4, no. 10, pp. 979–987, 2013.

[27] R. M. Goldstein and C. L. Werner, "Radar interferogram filtering for geophysical applications," *Geophysical Research Letters*, vol. 25, no. 21, pp. 4035–4038, 1998.

[28] O. Mora, J. J. Mallorqui, and A. Broquetas, "Linear and nonlinear terrain deformation maps from a reduced set of interferometric sar images," *IEEE Transactions on Geoscience and Remote Sensing*, vol. 41, pp. 2243–2253, 2003.

[29] R. F. Hanssen, *Radar Interferometry: Data Interpretation and Error Analysis (Vol. 2)*, Springer Science & Business Media, 2001.

[30] J. Li, W. Zheng, and X. Xu, "Information extraction and analysis of food disaster in Dongting Lake area base on sentinel-1," *Anhui Agricultural Science Bulletin*, vol. 26, pp. 151–153, 2020.

[31] H. El Kateb, H. Zhang, P. Zhang, and R. Mosandl, "Soil erosion and surface runoff on different vegetation covers and slope gradients: a field experiment in Southern Shaanxi Province, China," *Catena*, vol. 105, pp. 1–10, 2013.

[32] J. H. Xiao, S. X. Zhang, Y. Zhang, M. K. Li, and M. Hong, "Research on the response of land water reserve to rainfall in Yunnan Province," in *Proceedings of the 2019 China Earth Sciences Joint Academic Conference*, vol. 12, pp. 4–6, Beijing, China, 2019.

[33] L. Wang, J. Huang, Y. Du, Y. Hu, and P. Han, "Dynamic assessment of soil erosion risk using Landsat TM and HJ satellite data in Danjiangkou Reservoir Area, China," *Remote Sensing*, vol. 5, no. 8, pp. 3826–3848, 2013.

[34] S. Zhang and C. Zhu, "Soil loss and its effect on flooding catastrophe in Yangtze Drainage Basin," *Journal of Soil and Water Conservation*, vol. 15, pp. 9–13, 2001.

[35] W. F. Zhou, "Soil erosion and sediment deposition in Dongting Lake," *Water and Soil Conservation in China*, vol. 6, pp. 22–25+65, 1992.

[36] "Changjian water resources commission of the ministry of water resources," in *Annual Yangtze River Sediment Bulletin*, OLE, 2020, http://www.cjw.gov.cn/zwzc/bmgb/2020gb/49234.html.2020-07-31.

[37] Y. Zhou, J. Li, Y. Zhang, X. Zhang, and X. Li, "Enhanced lakebed sediment erosion in Dongting Lake induced by the operation of the Three Gorges Reservoir," *Journal of Geographical Sciences*, vol. 25, no. 8, pp. 917–929, 2015.

[38] Y. Du, H. P. Xue, S. J. Wu, F. Ling, F. Xiao, and X. H. Wei, "Lake area changes in the middle Yangtze region of China over the 20th century," *Journal of Environmental Management*, vol. 92, no. 4, pp. 1248–1255, 2011.

[39] B. Wang, F. Zheng, and Y. Guan, "Improved USLE-K factor prediction: a case study on water erosion areas in China," *International Soil and Water Conservation Research*, vol. 4, no. 3, pp. 168–176, 2016.

[40] C. G. Karydas, T. Sekuloska, and G. N. Silleos, "Quantification and site-specification of the support practice factor when mapping soil erosion risk associated with olive plantations in the Mediterranean island of Crete," *Environmental Monitoring and Assessment*, vol. 149, no. 1-4, pp. 19–28, 2009.